Gender-Specific Reproductive Tissue in Ratites and *Tyrannosaurus rex*

Mary H. Schweitzer,[1,2,3]* Jennifer L. Wittmeyer,[1] John R. Horner[3]

Unambiguous indicators of gender in dinosaurs are usually lost during fossilization, along with other aspects of soft tissue anatomy. We report the presence of endosteally derived bone tissues lining the interior marrow cavities of portions of *Tyrannosaurus rex* (Museum of the Rockies specimen number 1125) hindlimb elements, and we hypothesize that these tissues are homologous to specialized avian tissues known as medullary bone. Because medullary bone is unique to female birds, its discovery in extinct dinosaurs solidifies the link between dinosaurs and birds, suggests similar reproductive strategies, and provides an objective means of gender differentiation in dinosaurs.

A relatively small (femur length, 107 cm) *Tyrannosaurus rex* [Museum of the Rockies (MOR) specimen number 1125] was discovered at the base of the Hell Creek Formation (dated at ~70 million years ago) as an association of disarticulated elements with excellent preservation (*1*). At death, MOR 1125 was estimated to be 18 ± 2 years (*2*), on the basis of lines of arrested growth (LAG).

Interior femur fragments from MOR 1125 were reserved without preservatives for chemical and molecular analyses. Gross examination revealed a thin layer of bone tissue lining the inner (medullary) surfaces of the bone fragments that was structurally distinct from other described bone types (Fig. 1D) but possessed characteristics in common with avian medullary bone (MB).

MB is an ephemeral tissue, deposited on the endosteal surface of avian long bones (*3*–*10*). Its formation in female birds is triggered by increasing levels of gonadal hormones produced upon ovulation (*4*, *10*, *11*), but it can also be artificially induced in male birds by the administration of estrogen (*3*, *4*, *12*). Because MB is densely mineralized and extremely well vascularized, it provides an easily mobilized source of calcium necessary for the production of calcareous eggshells (*13*). We compare MB from emu and ostrich (*14*) at different stages of the laying cycle with newly identified dinosaur tissues, because these basal birds share more primitive features with nonavian dinosaurs than do extant neognaths (*15*–*18*).

Our investigations show that ratite MB differs from that seen in better-studied neognaths. We observed substantial variation between emu and ostrich MB tissues and between both ratites and reported neognath tissues (Fig. 1 and fig. S1). MB (Fig. 1) may be thick (chicken and ostrich) or quite thin (emu) at midshaft; and it may be separated by a distinct layer of endosteal laminar bone

[1]Department of Marine, Earth, and Atmospheric Sciences, North Carolina State University, Raleigh, NC 27695, USA. [2]North Carolina State Museum of Natural Sciences, Raleigh, NC 27601, USA. [3]Museum of the Rockies, Montana State University, Bozeman, MT 59717, USA.

*To whom correspondence should be addressed. E-mail: schweitzer@ncsu.edu

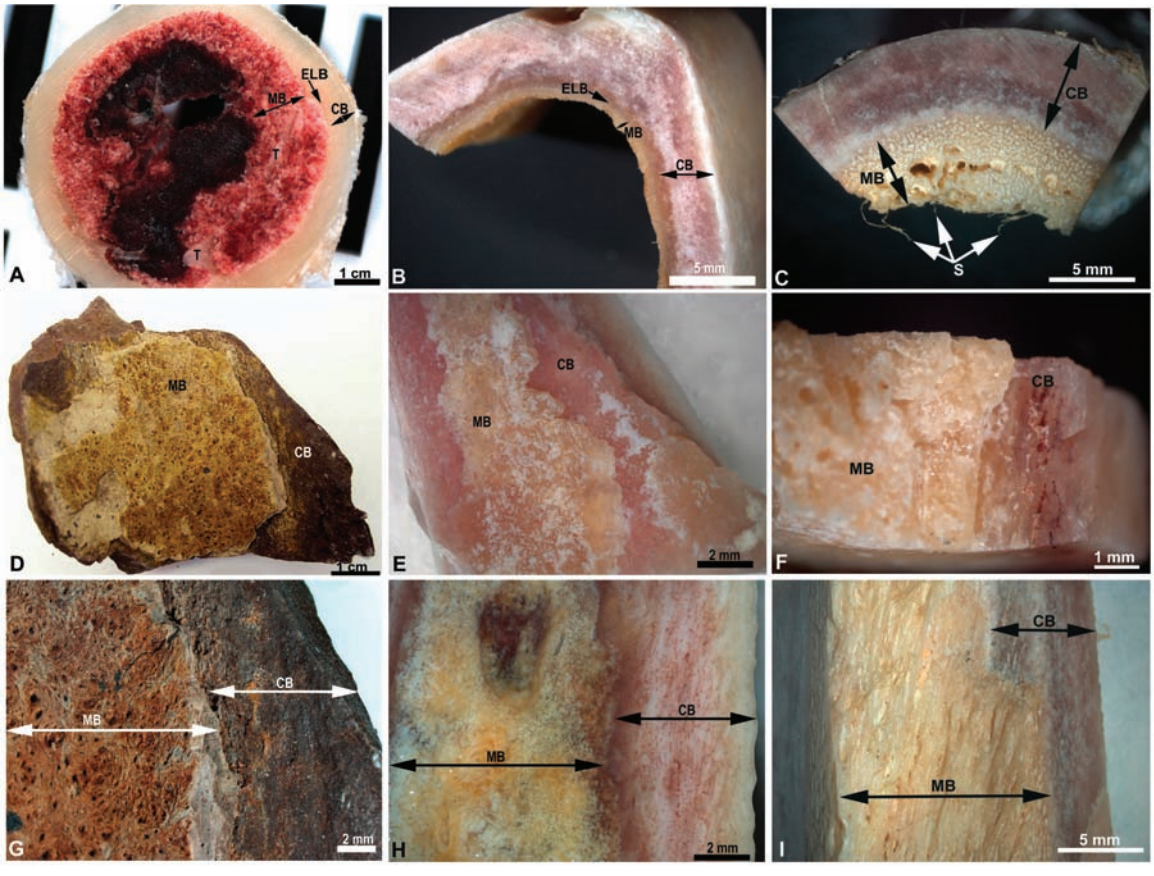

Fig. 1. Extant avian MB and homologous dinosaurian bone tissues. (**A**) Domestic laying hen, midshaft femur cross section showing the extension of spongy MB deep into the marrow cavity and surrounding preexisting trabeculae (T). (**B**) Laying emu, midshaft cross section, with a thin layer of MB on the endosteal bone surface, separated from overlying CB by ELB. (**C**) Ostrich MB arising from CB. Convoluted bony projections surround large cavities and form by continued deposition on hairlike spicules of calcified bone (S). (**D**) MB on endosteal surface of MOR 1125 femur fragment delineated from overlying CB by large vascular sinuses and change in color, texture, and density. (**E**) Emu and (**F**) ostrich bone taken at same aspect as (D), showing morphological distinction between bone types. (**G**) Higher magnification of dinosaur femur fragment in oblique view shows dense CB lined with newly described bone tissue, also seen in oblique view of emu (**H**) and ostrich (**I**) tibia. Ostrich MB is apparently unique in forming longitudinal tubules.

(ELB) as described by Chinsamy *et al*. (*19*) (chicken and emu), or not (ostrich). The innermost layer of MB in the ostrich [adjacent to the endosteal surface of cortical bone (CB)] appears to arise from dense sheets to form tubular structures that parallel the long axis of the bone (Fig. 1I). Thin hairlike spicules (Fig. 1C) of mineralized bone protrude from the tubes and may be intimately involved in their formation from the basal layer. Mineralized spicules were also noted arising from emu MB (fig. S2), but the tubelike structures were not so apparent or distinct. The MB tissues are morphologically distinct from overlying CB and are similarly distributed in both dinosaur (Fig. 1D) and ratite (Fig. 1, E and F) samples. Higher magnifications of *T. rex* (Fig. 1G) and ratite (Fig. 1, H and I) tissues show the open, crystalline, and fibrous structure of these highly vascular tissues, in contrast to the denser CB.

In a fresh fracture, dense and relatively homogenous dinosaur CB is distinct from the loosely organized and highly vascular MB internal to it (Fig. 2A). A distinct layer corresponding to ELB (*19*) separates the two bone types. A large erosion room is visible at this boundary, lined with laminar tissue. An emu bone fragment (Fig. 2B) in similar orientation shows MB tissues with a distinctive, less organized and "crumbly" texture relative to overlying CB. It is interspersed with or laid down between large erosion rooms within the deep cortex and ELB of the tibial shaft. The dense cortex and laminar structure of the ELB are easily distinguished from surrounding MB. The ostrich MB (Fig. 2C) differs in both texture and orientation, with open cavities that are bordered by tubelike bone spicules.

The lacy vascularity of the *T. rex* tissues (Fig. 2D) is consistent with the larger vascular canals and whorled pattern of the emu (Fig. 2E) and especially with the ostrich (Fig. 2F), where wide blood-filled sinuses separate forming bone spicules. In ground section (Fig. 2G), MOR 1125 femur cortical bone is characterized by well-developed multigeneration Haversian systems with obvious and defined cement lines, supporting a mature status for this dinosaur (*2*). A region of decreased vascularity and laminar structure marks the ELB. In contrast, the medullary tissues arising from the ELB are densely vascularized but show no evidence of Haversian remodeling or cement lines, indicating that this tissue is newly deposited, or younger bone. A fresh cut section of emu bone (Fig. 2H) in comparable orientation shows dense CB and vascular, crystalline, and loosely organized MB, separated by a thin, dense, and less vascular ELB. MB in the ostrich (Fig. 2I) is more extensive than in the emu samples, most likely because shelling had not yet begun (*14*). No distinct ELB is visible. MB appears laminar rather than spiculated in Fig. 2I, because the tubules formed by bony spicules are oriented longitudinally rather than in cross section as in Fig. 2F, but it is the same tissue.

Additional pattern similarities are seen in demineralized (*14*) ratite (Fig. 3, B and C) and *T. rex* (Fig. 3A) medullary tissues. In all cases, the matrix is fibrous and randomly organized. The reddish color in extant tissues is due to blood retained in sinuses that separate the bone spicules. The *T. rex* tissues are similarly pigmented, due either to diagenetic alteration or to close association of bony tissues with blood-producing marrow during the life of the dinosaur.

In all MB tissues shown, large vascular sinuses are easily discerned (Fig. 3, D to F), but in the *T. rex*, vascular openings are surrounded by circumferentially oriented matrix

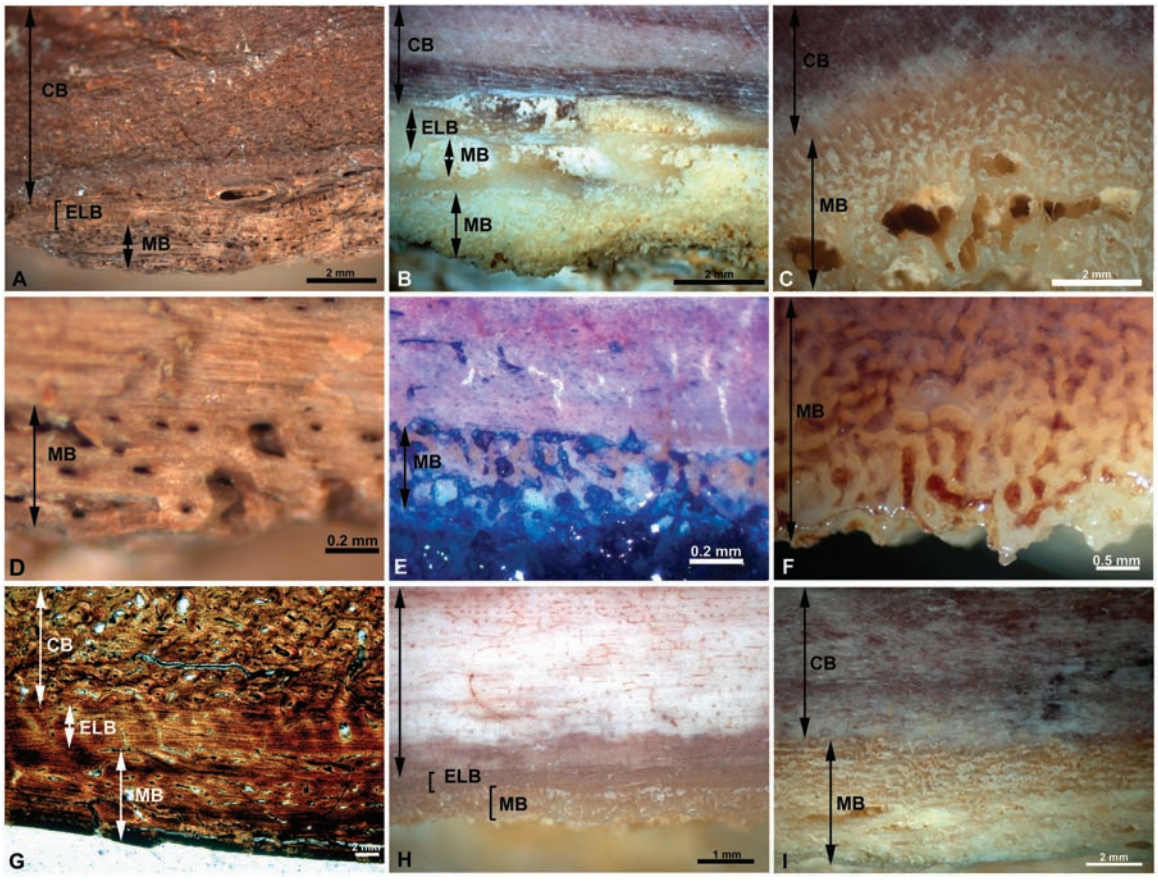

Fig. 2. Dinosaur and ratite comparative views. (**A**) Freshly broken fragment of MOR 1125 shows laminar ELB separating CB and MB. Bone tissues decrease in density internal to the ELB, because of increased vascularity. (**B**) Emu tibia, midshaft section. Erosion rooms extending into ELB are secondarily filled by MB. (**C**) Ostrich bone, midshaft. MB is distinct from CB, but no obvious ELB is visible and several large vascular sinuses are seen. (**D**) Higher magnification of MB region of MOR 1125, showing increased porosity and more random orientation of MB than CB or ELB. (**E**) Emu, stained (*14*) to distinguish bone from infiltrating marrow fat. MB is more vascular than overlying CB and exhibits a random, whorled pattern. (**F**) Ostrich MB, showing relationship of bony spicules to invading blood sinuses, colored red from remnant blood. (**G**) Ground section of MOR 1125. Dense cortical Haversian bone shows second- and third-generation remodeling. ELB separates Haversian bone from more vascular MB. (**H**) Similar orientation of emu femur shows dense CB, distinct ELB, and a thin layer of MB. (**I**) Ostrich MB appears more laminar than in (C) or (F) because of the longitudinal orientation of tubelike medullary spicules.

fibers (Fig. 3D) that are less apparent in extant bone. The ostrich medullary tissues are denser than either the emu (Fig. 3E) or *T. rex* samples, particularly closer to the cortex, but the variation in the size and density of vascular sinuses (Fig. 3F) is similar to that seen in the *T. rex* tissues. In planar view, MOR 1125 undemineralized tissues show a random orientation of fibers, and vascular openings penetrate deep into the tissues (Fig. 3G, inset) and exhibit an unusual doublet or triplet pattern, where multiple vessels penetrate an osteonlike core (arrows), also seen in the emu (Fig. 3H, arrows). The ostrich medullary tissues (Fig. 3I) are more variable, denser, and less random in appearance than those of the emu, but the morphology changes as the tissues extend into the medullary cavity. Close to the cortex (Fig. 3I, inset, and fig. S3), the bone is sheetlike, relatively dense, and punctured by vascular sinuses exhibiting the doublet pattern (arrows) noted above. As tissues extend into the medullary cavity (Fig. 3I), this pattern becomes obscured. Inset bone has been stained (*14*) for better contrast.

In regions of MOR 1125 bone where most of the medullary tissues have eroded (Fig. 3J), patches of denser CB can be seen, emphasizing the random mazelike pattern and large vascular sinuses of medullary tissues, a pattern also seen in the emu bone (Fig. 3K). The ostrich MB shows a similar pattern of bony spicules surrounding large and small blood sinuses (Fig. 3L).

Scanning electron micrographs (*14*) reveal the distinctive grainy texture and disorganized morphology of demineralized *T. rex* and avian MB (Fig. 4). This contrasts with the smooth and fibrous texture of demineralized CB from the same specimens (Fig. 4, E to H). Higher magnifications of demineralized CB (Fig. 4, I to K) emphasize the smooth, fibrous, and more ordered nature of all specimens, although in MOR 1125 (Fig. 4I), degradation is apparent.

MB occurs naturally only in extant female birds, although it varies in amount and distribution among taxa and with ovulatory phase (*5*, *20*). It is chemically, functionally, and structurally distinct from both overlying CB and internal trabecular bone (*21*, *22*). Although "medullary" and "trabecular" bone are terms often used interchangeably in the literature, MB has a larger surface area and is more vascular than other bone types, allowing rapid calcium mobilization (*5*). It is more highly mineralized, with a greater apatite-to-collagen ratio (*5*, *7*, *20*–*22*), and incorporates acidic mucopolysaccharides and glycosaminoglycans that are not present in CB (*5*, *11*). Additionally, the matrix of MB is higher in noncollagenous proteins and lower in collagen, and has a higher collagen III–to–collagen I ratio (*22*) relative to other bone types. If preservation allows, these characteristics will be used as part of ongoing research to chemically distinguish the two bone types in this dinosaur.

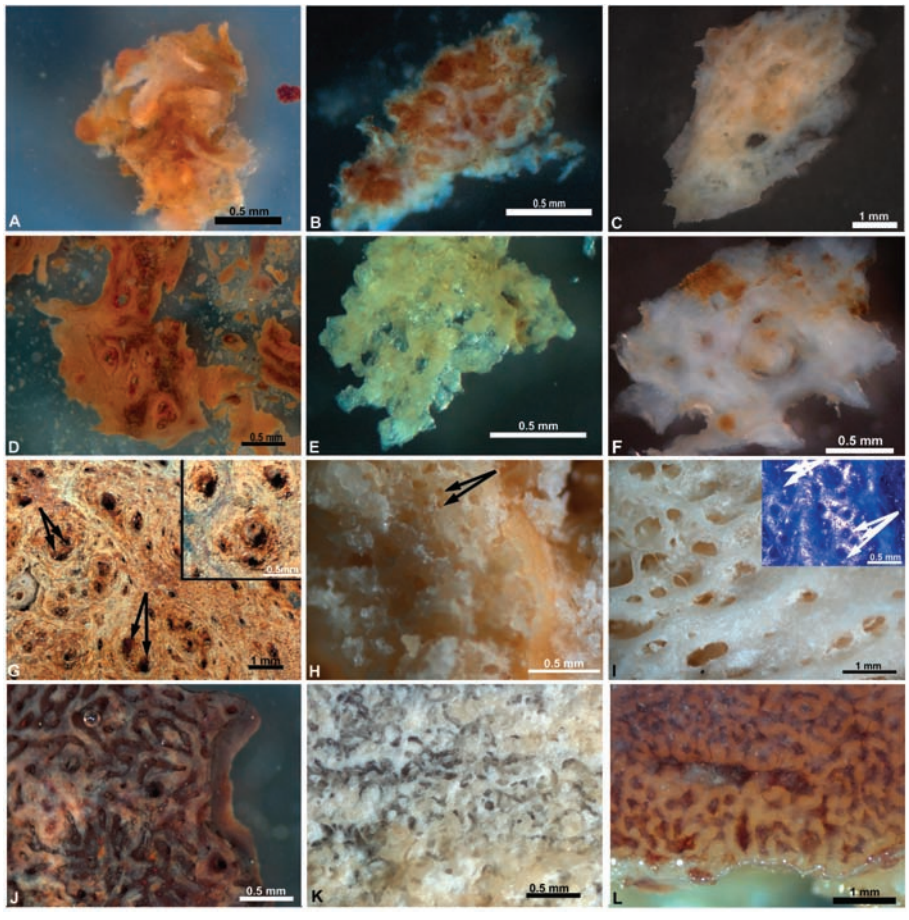

Fig. 3. Dinosaur and ratite MB. (**A**) MOR 1125, (**B**) emu, and (**C**) ostrich demineralized (*14*) MB. The coloration in (B) and (C) results from infiltration of tissues with blood sinuses. (**D**) MOR 1125, partially demineralized, showing enlarged, randomly arranged vascular openings surrounded by circumferential matrix fibers. Partially demineralized (**E**) emu and (**F**) ostrich medullary tissues show extensive vascular penetration, with randomly spaced and varyingly sized vessel openings. (**G**) Plane view of undemineralized dinosaur tissues shows fibrous matrix and an unusual pattern of vascular doublets or triplets within osteonlike structures (arrows). The inset shows variation in depth and diameter of vascular sinuses. (**H**) Undemineralized emu MB shows similar doublet pattern (arrows) and fibrous matrix. The greater depth of field makes focusing difficult. (**I**) Ostrich MB is denser closer to the cortex (inset), where the doublet/triplet pattern of vessels (arrows) is evident, but this becomes obscured by the increasing development of bony tubes and spicules as bone extends further into the medullary cavity. (**J**) Plane view of MOR 1125 shows the partially eroded, fibrous MB distributed across the cortex in a mazelike fashion. (**K**) Emu MB shows white (chloroform-altered) and cream-colored MB in the same mazelike pattern. (**L**) Thicker, randomly oriented tubular spicules of ostrich MB, showing deep penetration and intimate association of blood-containing sinuses.

The existence of avian-type MB in dinosaurs has been hypothesized (*9*, *23*) but not identified. In part, this could be because of taphonomic bias, because the death and fossilization of an ovulating dinosaur would be comparatively rare. Additionally, MB in extant birds is fragile, the spicules separating easily from the originating layer (fig. S1). Dinosaur MB may separate and be lost from overlying CB in a similar manner during diagenesis.

The location, origin, morphology, and microstructure of the new *T. rex* tissues support homology with ratite MB. The *T. rex* tissues line the medullary cavities of both femora of MOR 1125, suggesting an organismal response. The tissues are similar in distribution to those of extant ratites, being more extensive in proximal regions of the bone. They are clearly endosteal in origin, and the microstructure with large vascular sinuses is consistent with the function of MB as a rapidly deposited and easily mobilized calcium source. The random, woven character indicates rapidly deposited, younger bone. Finally, the robustly supported relationship between theropods and extant birds (*15*–*18*, *24*, *25*) permits the application of phylogenetic inference to support the identification of these tissues (*26*, *27*).

The morphology of these dinosaur tissues is not identical to that of extant neognaths

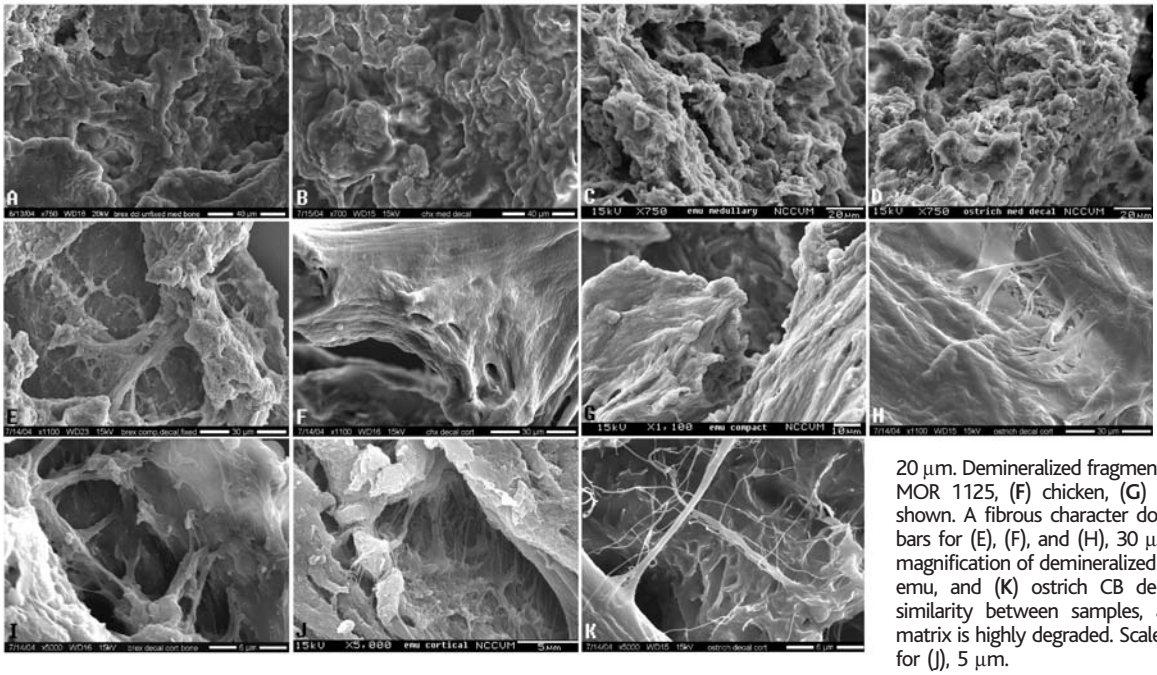

Fig. 4. Scanning electron microscope images of demineralized MB [(A) to (D)] and CB [(E) to (K)]. Demineralized, aldehyde-fixed (*14*) MB tissues from (**A**) MOR 1125, (**B**) extant laying hen, (**C**) emu, and (**D**) ostrich show random, crumbly texture. Organized collagen fiber bundles are not distinct in any sample because of rapid deposition and woven character. Scale bars for (A) and (B), 40 μm; for (C) and (D), 20 μm. Demineralized fragments of cortical bone from (**E**) MOR 1125, (**F**) chicken, (**G**) emu, and (**H**) ostrich are shown. A fibrous character dominates all samples. Scale bars for (E), (F), and (H), 30 μm; for (G), 10 μm. Higher magnification of demineralized CB from (**I**) MOR 1125, (**J**) emu, and (**K**) ostrich CB demonstrates the structural similarity between samples, although the MOR 1125 matrix is highly degraded. Scale bars for (I) and (K), 6 μm; for (J), 5 μm.

(fig. S1), but is more similar to that seen in ratites. *T. rex* medullary tissues are less extensive than those reported for neognaths, which may be explained by many factors. First, there is a wide range of MB morphologies in extant taxa (*20*), varying with both reproductive phase and the position of the egg within the reproductive tract (*6*). Medullary tissues become thinner as shelling progresses and disappear completely with deposition of the last egg. If the same was true of dinosaurs, MOR 1125 may have died toward the end of the laying cycle. Second, MB in extant birds is hypothesized to provide a buffer against excessive and debilitating bone resorption during shelling (*4*, *28*). It is most extensive in smaller taxa with high reproductive rates, because of the demand for rapid mobilization of skeletal calcium for shelling. Extinct theropods produced hard-shelled eggs, as did other dinosaurs and all extant birds (*29*, *30*). Although egg size is not known, eggs were most likely smaller relative to overall body size than in extant birds, resulting in less demand for bone calcium reserves and reducing the need to offset resorption. These factors may also contribute to the smaller ratio of medullary to cortical thickness in theropods than in extant birds. Finally, *T. rex*, although phylogenetically close to extant birds (*15*–*18*, *24*, *25*), was distinct in size, biomechanical constraints, and, to some degree, physiology (*31*); therefore, slight variations in bone and tissue types would be expected.

MB most likely first evolved within the lineage in early, small theropods with high productivity. A relatively thicker tyrannosaur bone cortex would reduce the need for MB, and its presence in MOR 1125 may reflect the retention of a primitive trait. This hypothesis may be tested by examination of the limb bones of the recently reported oviraptor containing eggs in the reproductive tract (*32*).

The existence of MB in crocodiles has been referred to anecdotally (*3*, *21*), but although they do resorb CB during shelling, experimental evidence suggests that they do not form MB (*6*, *9*, *11*, *12*), even after stimulation with estrogen (*33*). The identification of medullary tissues in dinosaurs supports a closer relationship to birds than to other extant archosaurs, sheds light on reproductive strategies of nonavian theropods, and provides an objective means of gender determination in extinct dinosaurs.

References and Notes

1. M. H. Schweitzer, J. L. Wittmeyer, J. R. Horner, J. A. Toporski, *Science* **307**, 1952 (2005).
2. J. R. Horner, K. Padian, *Proc. R. Soc. London Ser. B* **271**, 1875 (2004).
3. T. Yamamoto, H. Nakamura, T. Tsuji, A. Hirata, *Anat. Rec.* **264**, 25 (2001).
4. S. C. Miller, B. M. Bowman, *Dev. Biol.* **87**, 52 (1981).
5. C. G. Dacke *et al.*, *J. Exp. Biol.* **184**, 63 (1993).
6. M. A. Bloom, L. V. Domm, A. V. Nalbandov, W. Bloom, *Am. J. Anat.* **102**, 411 (1958).
7. T. G. Taylor, K. Simkiss, D. A. Stringer, in *Physiology and Biochemistry of the Domestic Fowl (Volume 2)*, D. J. Bell, B. M. Freeman, Eds. (Academic Press, London, 1971), pp. 621–640.
8. E. Bonucci, G. Gherardi, *Cell Tissue Res.* **163**, 81 (1975).
9. A. Chinsamy, P. M. Barrett, *J. Vertebr. Paleontol.* **17**, 450 (1997).
10. A. Ascenzi, C. Francois, D. S. Bocciarelli, *J. Ultrastruct. Res.* **8**, 491 (1963).
11. T. Sugiyama, S. Kusuhara, *Asian-Australas. J. Anim. Sci.* **14**, 82 (2001).
12. T. Ohashi, S. Kusuhara, K. Ishida, *Br. Poult. Sci.* **28**, 727 (1987).
13. J. L. Arias, M. S. Fernandez, *World's Poult. Sci. J.* **57**, 349 (2001).
14. Materials and methods are available as supporting material on *Science* Online.
15. J. A. Gauthier, *Mem. Calif. Acad. Sci.* **8**, 1 (1986).
16. L. M. Chiappe, *Nature* **378**, 349 (1995).
17. K. Padian, L. M. Chiappe, *Sci. Am.* **278**, 38 (1998).
18. J. Cracraft, J. A. Clarke, in *New Perspectives on the Origin and Early Evolution of Birds. Proceedings of the International Symposium in Honor of J. H. Ostrom*, J. Gauthier, L. F. Gall, Eds. (Special Publication of the Peabody Museum of Natural History, New Haven, CT, 2001), pp. 143–147.
19. A. Chinsamy, L. M. Chiappe, P. Dodson, *Paleobiology* **21**, 561 (1995).
20. H. Schraer, S. J. Hunter, *Comp. Biochem. Physiol. A* **82**, 13 (1985).
21. C. C. Whitehead, *Poult. Sci.* **83**, 193 (2004).
22. L. Knott, A. J. Bailey, *Br. Poult. Sci.* **40**, 371 (1999).
23. D. M. Martill, M. J. Barker, C. G. Dacke, *Nature* **379**, 778 (1996).
24. C. A. Forster, S. D. Sampson, L. M. Chiappe, D. W. Krause, *Science* **279**, 1915 (1998).
25. P. C. Sereno, *Annu. Rev. Earth Planet. Sci.* **25**, 435 (1997).
26. H. N. Bryant, A. P. Russell, *Philos. Trans. R. Soc. London Ser. B* **337**, 405 (1992).
27. L. M. Witmer, in *Functional Morphology in Vertebrate Paleontology*, J. J. Thomason, Ed. (Cambridge Univ. Press, New York, 1995), pp. 19–33.
28. S. Wilson, B. H. Thorpe, *Calcif. Tissue Int.* **62**, 506 (1998).
29. K. Carpenter, Ed., *Eggs, Nests, and Baby Dinosaurs: A Look at Dinosaur Reproduction* (Indiana Univ. Press, Bloomington, IN, 1999).
30. K. E. Mikhailov, *Spec. Pap. Palaeontol.* **56**, 1 (1997).
31. M. H. Schweitzer, C. L. Marshall, *J. Exp. Zoolog. Part B Mol. Dev. Evol.* **291**, 317 (2001).
32. T. Sato, Y. Chang, X. Wu, D. Zelenitsky, Y. Hsiao, *Science* **308**, 375.
33. R. M. Elsey, C. S. Wink, *Comp. Biochem. Biophys.* **84A**, 107 (1986).

34. We thank C. Ancell, J. Barnes, D. Enlow, J. Flight, A. Friederichs, B. Harmon, L. Knott, E. Lamm, N. Myrhvold, A. de Ricqles, A. Steele, and T. Sugiyama for insight and assistance, and D. Brown (Carlhaven Farms) and J. Perkins (Perkins Ostrich) for ratite specimens. R. Avci (Image and Chemical Analysis Laboratory, Montana State University) and M. Dykstra [Laboratory for Advanced Electron and Light Optical Methods, North Carolina State University (NCSU) College of Veterinary Medicine] provided scanning electron micro-

scope access. We also thank J. Fountain and K. Padian for editorial advice. The ground section of MOR 1125 was provided by Quality Thin Sections, and the laying hen demineralized thin sections were provided by J. Barnes (NCSU College of Veterinary Medicine). Site access was provided by the Charles M. Russell National Wildlife Refuge. The research was funded by NCSU as well as by grants from N. Myhrvold (J.R.H.) and NSF (M.H.S.).

Supporting Online Material
www.sciencemag.org/cgi/content/full/308/5727/1456/DC1
Materials and Methods
Figs. S1 to S3

11 March 2005; accepted 21 April 2005
10.1126/science.1112158

Ivory-billed Woodpecker (*Campephilus principalis*) Persists in Continental North America

John W. Fitzpatrick,[1]* Martjan Lammertink,[1,2] M. David Luneau Jr.,[3] Tim W. Gallagher,[1] Bobby R. Harrison,[4] Gene M. Sparling,[5] Kenneth V. Rosenberg,[1] Ronald W. Rohrbaugh,[1] Elliott C. H. Swarthout,[1] Peter H. Wrege,[1] Sara Barker Swarthout,[1] Marc S. Dantzker,[1] Russell A. Charif,[1] Timothy R. Barksdale,[6] J. V. Remsen Jr.,[7] Scott D. Simon,[8] Douglas Zollner[8]

The ivory-billed woodpecker (*Campephilus principalis*), long suspected to be extinct, has been rediscovered in the Big Woods region of eastern Arkansas. Visual encounters during 2004 and 2005, and analysis of a video clip from April 2004, confirm the existence of at least one male. Acoustic signatures consistent with *Campephilus* display drums also have been heard from the region. Extensive efforts to find birds away from the primary encounter site remain unsuccessful, but potential habitat for a thinly distributed source population is vast (over 220,000 hectares).

The ivory-billed woodpecker is one of seven North American bird species that are suspected or known to have become extinct since 1880 (*1*). One of the world's largest woodpeckers, this species of considerable beauty and lore was uncommon but widespread across lowland primary forest of the southeastern United States until midway through the 19th century (*2*, *3*). Its disappearance coincided with the systematic annihilation of virgin tall forests across the southeastern United States between 1880 and the 1940s. Relentless pursuit by professional collectors accelerated the species' decline from 1890 to the early 1920s. The last well-documented population occupied a stand of old-growth bottomland hardwood forest in northeastern Louisiana (the Singer Tract) during the late 1930s (*3*–*6*). That population disappeared as the Singer Tract was logged amid cries for protection of both forest and bird. The final individual in the Singer Tract, an unpaired female, was last seen in cut-over forest remnants in 1944 (*7*).

A resident subspecies of ivory-billed woodpecker (*Campephilus principalis bairdii*) occupied tall forests throughout Cuba, and a small population was mapped and photographed in eastern Cuba as late as 1956 (*8*). Fleeting observations of at least two individuals in 1986 and 1987 by several experts are widely accepted as valid (*9*), but repeated efforts to confirm the continued existence of that population have failed (*10*).

Anecdotal reports of ivory-billed woodpeckers in the southern United States continue to this day. Such reports are suspect because of the existence and relative abundance throughout this region of the superficially similar pileated woodpecker (*Dryocopus pileatus*). Three reports were accompanied by physical evidence, but their veracity continues to be questioned [supporting online material (SOM) text]. Thus, no living ivory-billed woodpecker has been conclusively documented in continental North America since 1944.

At approximately 13:30 Central Standard Time (CST) on 11 February 2004, while kayaking alone on a bayou in the Cache River National Wildlife Refuge, Monroe County, Arkansas, G. Sparling spotted an unusually large red-crested woodpecker flying toward him and landing near the base of a tree about 20 m away. Several field marks suggested that the bird was a male ivory-billed woodpecker (SOM text), and Sparling hinted at his sighting on a Web site. T. Gallagher and B. Harrison were struck by the apparent authenticity of this sighting and arranged to be guided through the region by Sparling. At 13:15 CST on 27 February 2004, within 0.5 km of the original sighting, an ivory-billed woodpecker (sex unknown) flew directly in front of their canoe with the apparent intention of landing on a tree near the canoe, thereby fully revealing its dorsal wing pattern. The bird instead veered into the forest, apparently landed briefly several times (each time blocked from the observers' sight by trees), and then flew off (SOM text and fig. S1). Efforts to locate the bird over the next several days failed, but subsequent surveys by teams of experienced observers yielded a minimum of five additional visual encounters between 5 April 2004 and 15 February 2005 (SOM text). All seven convincing sightings were within 3 km of one another.

At 15:42 Central Daylight Time on 25 April 2004, M. D. Luneau secured a brief but crucial video of a very large woodpecker perched on the trunk of a water tupelo (*Nyssa aquatica*), then fleeing from the approaching canoe (fig. S2 and movie S1). The woodpecker remains in the video frame for a total of 4 s as it flies rapidly away. Even at its closest point, the woodpecker occupies only a small fraction of the video. Its images are blurred and pixilated owing to rapid motion, slow shutter speed, video interlacing artifacts, and the bird's distance beyond the video camera's focal plane. Despite these imperfections, crucial field marks are evident both on the original and on deinterlaced and magnified video fields (*11*) (fig. S3). At least five diagnostic features allow us to identify the subject as an ivory-billed woodpecker.

1) Size. When the woodpecker first begins to take flight from the left side of a tupelo trunk, two video fields reveal the dorsal surface of the right wing and a large black tail (Fig. 1). The minimum distances between the "wrist" and the tip of its tail—measured independently on each of the two video fields and compared to known scales (the diameter of the tupelo trunk at two places)—are 34 to 38 cm. These values exceed comparable values for the pileated woodpecker and correspond to the upper range for the ivory-billed woodpecker (fig. S4).

[1]Cornell Laboratory of Ornithology, Cornell University, 159 Sapsucker Woods Road, Ithaca, NY 14850, USA. [2]Institute for Biodiversity and Ecosystem Dynamics, Universiteit van Amsterdam, Mauritskade 61, 1092 AD Amsterdam, Netherlands. [3]Department of Engineering Technology and Department of Information Technology, University of Arkansas at Little Rock, Little Rock, AR 72204, USA. [4]Department of Communications, Oakwood College, Huntsville, AL 35896, USA. [5]107 Stillmeadow Lane, Hot Springs, AR 71913, USA. [6]Birdman Productions, Post Office Box 1124, 65 Mountain View Drive, Choteau, MT 59422, USA. [7]Museum of Natural Science, Louisiana State University, Baton Rouge, LA 70803, USA. [8]The Nature Conservancy, Arkansas Chapter, 601 North University Avenue, Little Rock, AR 72205, USA.

*To whom correspondence should be addressed. E-mail: jwf7@cornell.edu